GNSS processing using Kalman Filter on Lie Groups

Marcos R. Fernandes *, **Giorgio M. Magalhães** *,
Yusef Cáceres *, **João B. R. do Val** *

* *State University of Campinas*
School of Electric and Computer Engineering.
(e-mail: marofe@dt.fee.unicamp.br, giorgio08@gmail.com,
yusefc@gmail.com,jbosco@unicamp.br)

Abstract
This paper explores the problem of position and speed estimation of a target using satellite-based measurements in a Lie Group Kalman-like filter. The filter employs an intrinsic formulation of a nearly constant velocity model based on the Frenet-Serret frame, embedded in a Lie Group structure. It stands as a more suitable model for the kinematics of a target in space than the usual Euclidean model since it induces a banana-shaped distribution instead of the typical ellipsoidal provided by Gaussian schemes. The paper presents numeric experiments using a real application dataset to evaluate the proposed filtering scheme's performance against the standard Euclidean representation approach. A differential GNSS solution provided by commercial software furnishes the ground truth. The results indicate a better performance of the proposed Lie Groups filtering scheme.

Keywords: Satellite-based navigation, Lie Groups, Kalman Filter.

Today's most commonly used navigation system is the *Global Navigation Satellite System* (GNSS). It consists of different constellations of satellites such as GPS, GLONASS, Beidou, and Galileo (Subirana et al., 2013). The main advantage of satellite-based navigation is that it provides absolute positioning and global coverage with long-term accuracy. Moreover, due to its relatively low cost, this type of navigation is primarily adopted for commercial use (Farrell, 2008).

The GNSS positioning principle relies on solving a geometric problem involving a user's distances (ranges) to a set of at least four satellites with known coordinates (Groves, 2013). The usual approach to obtaining a trajectory solution is using the Kalman Filter. The satellite measurements are combined with a prior kinematic model to yield the final solution in this approach.

Existent methods for solving the GNSS include the premise that the system state follows a Gaussian distribution with a representation in the Euclidean space. Some examples are (Pulford, 2010; Takasu and Yasuda, 2007; Sahmoudi and Landry, 2009). However, recent works have shown that banana-shaped distributions for some systems, such as differential-drive robots (Long et al., 2012) and aerial targets (Magalhães et al., 2018) and aerial targets more appropriately represent the uncertainty in their movements.

For these cases, the Gaussian assumption can compromise the filtering performance. In addition, (Long et al., 2012) shows that although the use of exponential coordinates yields a banana-shaped distribution in the Lie group, the distribution in the respective algebra remains Gaussian. Therefore, a representation of the system state in a matrix Lie group structure instead of the Euclidean space is bound to render a more suitable approach for scenarios in which a rigid body performs simultaneous translations and rotations.

Especially for aerial vehicle applications, e.g., drones and airplanes, it is reasonable to expect that the state distribution is banana-shaped. As described in detail in (Magalhães, 2021) for radar tracking application, the curved shape of the state distribution could better explain the simultaneous existence of uncertainties in speed and angular velocity of the target movement.

Besides, filtering strategies usually neglect the geometrical constraints associated with the system, while Lie group-based filters can naturally consider such restrictions (Barrau and Bonnabel, 2020).

From this standpoint, one can expect that the GNSS processing could also benefit from the Lie group structure to represent the kinematic states. Accordingly, this work proposes applying the Lie group theory to the GNSS processing problem to leverage the advantages above of the Lie Group to satellite-based navigation systems.

More specifically, an intrinsic formulation of a nearly constant velocity model is adopted based on the Frenet-Serret frame. A matrix Lie Group accommodates the uncertainties on position, speed, and the Frenet-Serret frame orientation. After that, the filter is developed directly on Lie groups. The noise considered is Gaussian in the Lie algebra space, which induces a banana-shaped distribution in the Lie group.

In the literature, one can find applications of the Lie Group framework that combines GNSS solution (processed

ISSN: 2525-8311 0724 DOI: 10.20906/CBA2022/3274

separately with a Euclidean filter) with other sensors such as IMU, cameras, Lidar, etc. (see (Cui, 2021; Barczyk and Lynch, 2013; Barrau and Bonnabel, 2018)). However, to the best of the authors' knowledge, this is the first work that directly employs a Lie Group structure on raw GNSS data processing.

Finally, we compare the classic Kalman filter and the one proposed here using raw data from a GNSS receiver installed on a hexacopter. The performance is evaluated in the position Root Mean Squared Error (RMSE) terms. As ground truth, we consider the GNSS differential solution from the commercial software Inertial Explorer®, which provides centimeter-level precision.

This paper reads as follows. Section 1 briefly introduces the main concepts of the Lie groups theory and filtering algorithms on Lie Groups. Section 2 presents the equations regarding the GNSS measurements. Section 3 describes an intrinsic formulation of a nearly constant velocity model on Lie Groups. This topic is followed by experimental evaluations using a real dataset in Section 5. Concluding remarks are provided in Section 6.

1. KALMAN FILTERING ON LIE GROUPS

1.1 Lie Group Theory

A Lie group is a mathematical structure that joins the concept of a differentiable manifold with the idea of a group (Hall, 2007). It is defined as a group whose set G has the structure of a smooth manifold so that the group operation is differentiable. The group elements are invertible square matrices for a matrix Lie Group, and the group operation is the usual matrix product.

A Lie algebra is a vector space equipped with the so-called *Lie bracket* product $[\![\cdot,\cdot]\!]$. The importance of the Lie algebra lies in the fact that most of the properties of the Lie group come from properties in the Lie algebra. In addition, the vector space properties of the Lie algebra enable a more convenient framework to perform many of the manipulations on Lie group elements. For matrix Lie groups, the associated Lie algebra is the vector space of square matrices, and the Lie bracket is the commutator $[\![X,Y]\!] = XY - YX$.

The *exponential map* establishes the relationship between the Lie group and its Lie algebra. For the matrix Lie group, it reduces to the matrix exponential. Specifically, let G be a matrix Lie group and let $\mathfrak{g}$ be its Lie algebra, the exponential map $\exp_G : \mathfrak{g} \to G$ is given by $g = \exp_G(X) = \sum_{k=0}^{\infty} \frac{1}{k!} X^k$ where $X \in \mathfrak{g}$ and $g \in G$.

In general, the exponential map is not bijective. However, it is possible to show that there exist open neighborhoods of the identity element I on the Lie group and of the identity element 0 on the Lie algebra for which the exponential map is a diffeomorphism [1]. Restricted to these open sets, we define the *logarithm map* $\log_G : G \to \mathfrak{g}$ as the inverse of the exponential map.

[1] A diffeomorphism is an isomorphism between differentiable manifolds. A differentiable invertible function between manifolds with differentiable inverse.

Since the Lie algebra is a vector space, it can represent any of its elements in the form, $X = \sum_{i=1}^{p} x_i E_i$ where $X \in \mathfrak{g}$, $x_i \in \mathbb{R}$ and $\mathcal{B} = \{E_1, \ldots, E_p\}$ form a basis for the Lie algebra. The value p is said to be the dimension of the Lie Group.

Therefore, when working on the Lie algebra, instead of manipulating the elements X as matrices, one can work with the *exponential coordinates* x_i associated with the basis $\mathcal{B}$. With that in mind, the coefficients are written as a vector $x = [x_1, \ldots, x_p]^T$, and the following isomorphism is defined,

$$\begin{aligned} [\cdot]_G^\vee : \mathfrak{g} &\to \mathbb{R}^p & [\cdot]_G^\wedge : \mathbb{R}^p &\to \mathfrak{g} \\ X &\mapsto [X]_G^\vee & x &\mapsto [x]_G^\wedge \end{aligned} \tag{1}$$

For brevity, the following notations are used hereafter,

$$\exp_G^\wedge(x) := \exp_G([x]_G^\wedge), \tag{2}$$

$$\log_G^\vee(g) := [\log_G(g)]_G^\vee \tag{3}$$

where $x \in \mathbb{R}^p$ and $g \in G$.

The exponential map can be interpreted as a parameterization for the Lie Group in local coordinates around the identity element. This parameterization can be extended to the neighborhood of any element $\mu \in G$ in a connected Lie group using the *Left Translation* as follows, $\mathscr{L}_\mu(\epsilon) := \mu \exp_G^\wedge(\epsilon), \forall \epsilon \in \mathbb{R}^p$. Since the exponential map is locally a diffeomorphism, there exist open neighborhoods of $\mu \in G$ and of $\mathbf{0}$ in $\mathbb{R}^p$ for which this parameterization is one-to-one.

The Lie theory also defines two adjoint representations. The first one represents the Lie group on its Lie algebra, i.e. it is the linear map that takes an element of the Lie group to a linear transformation in the Lie algebra, and it is defined as (see (Chirikjian, 2011))

$$\mathrm{Ad}_G(g)y = \left[g[y]_G^\wedge g^{-1}\right]_G^\vee \tag{4}$$

where $g \in G$, $y \in \mathbb{R}^p$. The second adjoint representation is the representation of the Lie algebra on itself so that each element of the Lie algebra defines a linear transformation in the Lie algebra. This adjoint representation is defined by the Lie bracket (Chirikjian, 2011) in the form

$$\mathrm{ad}_G(x)y = \left[[x]_G^\wedge [y]_G^\wedge - [y]_G^\wedge [x]_G^\wedge\right]_G^\vee \tag{5}$$

where $x, y \in \mathbb{R}^p$.

Furthermore, in many applications of the Lie group, particularly in filtering, one is interested in analyzing the behavior of a Lie group element $g \in G$ as a function of time and, naturally, it's derivative regarding time, $\dot{g}(t)$. From the theory of differential manifolds, $\dot{g}(t)$ is a vector in the vector space tangent to the Lie group G at the element $g(t)$, i.e. $\dot{g}(t) \in T_{g(t)}G$.

If we consider a local parameterization in the form $g = \exp_G^\wedge(x)$, then the relation between the time variation of g to the time variation of the local coordinates x, represented in the Lie algebra, as follows,

$$g^{-1}\dot{g} = [J_r(x)\dot{x}]_G^\wedge \tag{6}$$

where $J_r(x)$ is refereed in the literature as *right-Jacobian matrix* (Chirikjian, 2011) and it is computed as

$$J_r(x) = \sum_{k=0}^{\infty} \frac{(-1)^k}{(k+1)!} \mathrm{ad}_G(x)^k. \tag{7}$$

ISSN: 2525-8311 0725 DOI: 10.20906/CBA2022/3274

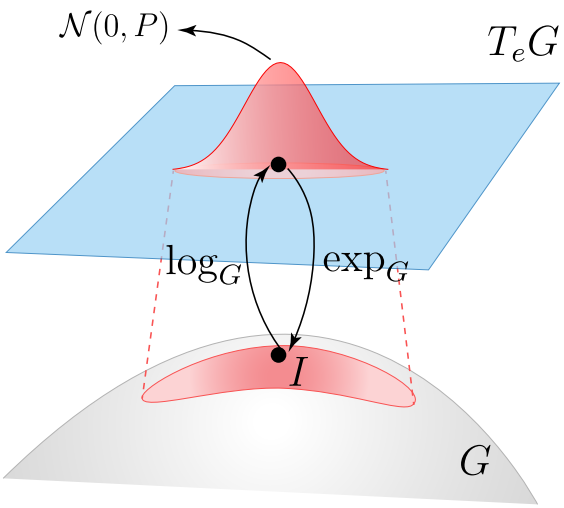

Figure 1. Concentrated Gaussian Distribution in the neighborhood of the identity element. Note the curved shape on the Lie Group but Gaussian in the tangent space.

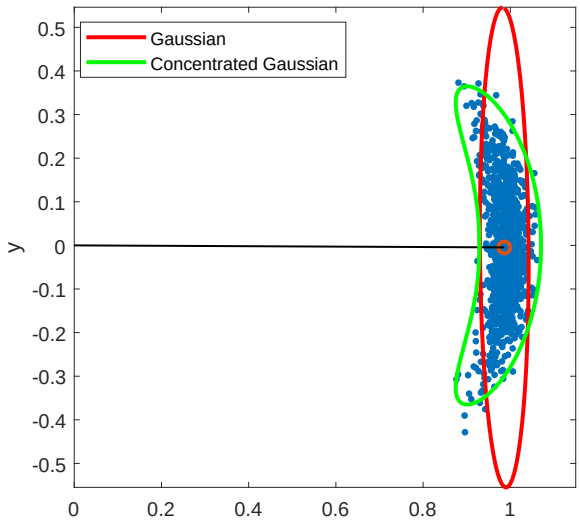

Figure 2. Comparison between the usual Gaussian and the Concentrated Gaussian distribution. Notice that the CGD shows a banana-shaped form while the Gaussian has an ellipsoidal shape.

1.2 Random Variables on Lie Group

Given a Matrix Lie Group $G \subseteq \mathbb{R}^{n\times n}$, a random matrix $X \in G$ with pdf $p(X)$, mean $\mu \in G$ and covariance $P = P^\intercal \succ 0$ is defined by

$$0_{n\times n} = \int_G \log_G^\vee(\mu^{-1}X)p(X)dX, \tag{8}$$

$$P = \int_G \log_G^\vee(\mu^{-1}X)\log_G^\vee(\mu^{-1}X)^\intercal p(X)dX. \tag{9}$$

From this standpoint, the concept of *Concentrated Gaussian Distribution* (CGD) (Bourmaud et al., 2014) is used to define a probability density tailored to matrix Lie groups. The mean is defined in the group and the covariance in the Lie algebra. Accordingly, a random variable on a matrix Lie group is expressed as

$$X = \mu \exp_G^\wedge(\epsilon), \quad \epsilon \sim \mathcal{N}(0,P), \tag{10}$$

and the pdf of X takes the form

$$p(X) := \alpha \exp\left(-\frac{1}{2}\|\log_G^\vee(\mu^{-1}X)\|^2_{P^{-1}}\right) \tag{11}$$

where $\alpha \in \mathbb{R}$ is a normalizing factor.

Let $\epsilon = \log_G^\vee(\mu^{-1}X)$ and assume that P has small eigenvalues, then the probability $p(\mu\exp_G^\wedge(\epsilon))$ presents a mass concentrated around the group identity. In this case, the distribution of ϵ in the Lie Algebra becomes the classical Gaussian distribution, i.e. $\epsilon \sim \mathcal{N}(0,P)$. In correspondence, the distribution of X is called a *Concentrated Gaussian Distribution* (CGD) on G and it is denoted by $X \sim \mathcal{N}_G(\mu,P)$. Fig. 1 illustrates the tangent space and the respective Gaussian distribution mapped to the Lie Group. Note that the element from the tangent space is mapped to the group through the exponential map, which results in a curved distribution. The CGD requires the Lie group to be unimodular and connected to allow the shift of any element in the group via the group translation (Bourmaud et al., 2013).

Figure 2 shows a Monte Carlo simulation of a random variable following a CGD. Note that, as expected, the samples form a banana-shaped cloud.

1.3 Dynamic System

Once a r.v. is defined on a Lie Group, a stochastic dynamic system can be modeled such that its states are embedded on a matrix Lie Group G. Let $X \in G \subseteq \mathbb{R}^{n\times n}$ be the system state. Let the following stochastic differential equation express the system state evolution,

$$\dot{X} = X[\Omega(X,u) + w]_G^\wedge \tag{12}$$

where $\Omega : G \times \mathbb{R}^m \to \mathbb{R}^p$ is *the left velocity function* and w is a multidimensional white noise with covariance Q_c. Also, consider that measurements are available in discrete-time instants in the form

$$y_{k+1} = h(X_k) + \nu_k \tag{13}$$

where $y_k \in \mathbb{R}^m$ is the measurement vector, $h : G \to \mathbb{R}^m$ is the measurement model and $\nu_k \overset{iid}{\sim} \mathcal{N}(0,R_k)$ is the measurement noise. For a small sample time Δt, the discrete form of the dynamic system Eq. (12) can be approximated as,

$$X_{k+1} = X_k \exp_G^\wedge\left(\Omega(X_k,u_k)\Delta t + w_k\right), \tag{14}$$

where $w_k \overset{iid}{\sim} \mathcal{N}(0,Q_k)$ and $Q_k = Q_c\Delta t$. For convenience, denote $\Omega_k := \Omega(X_k,u_k)\Delta t$.

1.4 Kalman Filter on Lie Groups

Based on the definition of r.v. and stochastic dynamic system on Lie Groups, one can employ the Kalman Filtering framework to generate estimates of a dynamic system state evolving on a Lie Group. The Discrete Extended Kalman Filter (D-EKF) on Lie Group (Bourmaud et al., 2013, 2016) is summarized by the following equations,

ISSN: 2525-8311 0726 DOI: 10.20906/CBA2022/3274

$$\hat{X}_{k+1|k} = \hat{X}_{k|k} \exp_G^{\wedge}(\hat{\Omega}_k), \tag{15a}$$
$$P_{k+1|k} = \mathscr{F} P_{k|k} \mathscr{F}^{\intercal} + J_r(\hat{\Omega}_k) Q_k J_r(\hat{\Omega}_k)^{\intercal} \tag{15b}$$
$$K = P_{k+1|k} \mathscr{H}^{\intercal} (R_{k+1} + \mathscr{H} P_{k+1|k} \mathscr{H}^{\intercal})^{-1} \tag{15c}$$
$$\hat{X}_{k+1|k+1} = \hat{X}_{k+1|k} \exp_G^{\wedge}(K \log_{G'}^{\vee}[h(\hat{X}_{k+1|k})^{-1} y_{k+1}]) \tag{15d}$$
$$P_{k+1|k+1} = (I - K\mathscr{H}) P_{k+1|k} (\bullet)^{\intercal} + K R_{k+1} K^{\intercal} \tag{15e}$$

where

$$\mathscr{F} := \mathrm{Ad}_G(\exp_G^{\wedge}(-\hat{\Omega}_k)) + J_r(\hat{\Omega}_k)\mathscr{C}_k \tag{15f}$$
$$\mathscr{C}_k := \frac{\partial}{\partial \epsilon}[\Omega(\hat{X}_{k|k} \exp_G^{\wedge}(\epsilon))]\Big|_{\epsilon=0} \tag{15g}$$
$$\mathscr{H} := \frac{\partial}{\partial \epsilon} \log_G^{\vee}[h(\hat{X}_{k+1|k})^{-1} h(\hat{X}_{k+1|k} \exp_G^{\wedge}(\epsilon))]\Big|_{\epsilon=0}. \tag{15h}$$

2. GNSS MODEL

The basic measurement provided by a GNSS system is the travel time δT of the signal to propagate from the phase center of the satellite antenna (the emission time) to the phase center of the receiver antenna (the reception time). This value multiplied by the speed of light gives the apparent range $\rho = c\delta T$ between them. This measurement is what is known as the *pseudo-range* (Subirana et al., 2013). It is called pseudo-range because it does not match the geometric distance due to, among other factors, atmosphere-induced delays and time synchronization errors between receiver and satellite clocks. The actual *geometric range* ($\bar{\rho}$) is the Euclidean distance between the satellite and receiver antenna.

Therefore, the *pseudo-range measurement* (ρ) obtained by the receiver includes, besides the geometric range, other terms such as the ionosphere and troposphere delay, relativistic effects, and instrumental delays (of satellite and receiver), multipath and receiver noise. Taking explicitly into account all these terms, as in (Subirana et al., 2013), the pseudo-range model from the i-th visible satellite can be stated as follows

$$\rho^i = \bar{\rho}^i + \delta\rho^i_{\mathrm{rel}} + c\Delta T^i + Tr^i + I^i + TGD^i + \epsilon^i \tag{16}$$

where

$$\bar{\rho}^i = \|p^i_{\mathrm{sat}} - p\|_2 \tag{17a}$$
$$\Delta T^i = \Delta t_{\mathrm{rcv}} - \Delta t^i_{\mathrm{offset}} - \Delta t^i_{\mathrm{rel}} \tag{17b}$$

Here, p^i_{sat} stands for the i-th satellite position, p is the desired receiver position, Δt_{rcv} is the receiver clock synchronization error, $\Delta t^i_{\mathrm{offset}}$ is the satellite clock drift, TGD^i is the Total Group Delay and ϵ^i is a white noise accounting for multipath and receiver noise, $\delta\rho^i_{\mathrm{rel}}$ and $\Delta t^i_{\mathrm{rel}}$ are the range and clock errors due to relativistic effects, respectively, which are calculated from the satellite orbit. Furthermore, Tr^i and I^i stand for the troposphere and ionospheric effects. These effects are the main source of accuracy degradation in the GNSS measurements for open sky applications.

The troposphere-induced error depends on the temperature, pressure, humidity, time of the day, and transmitter and receiver locations. In contrast, the ionospheric induced error depends on the electron density in the atmosphere, which is typically driven by sun radiation. Fortunately, both troposphere and ionospheric effects can be partially mitigated

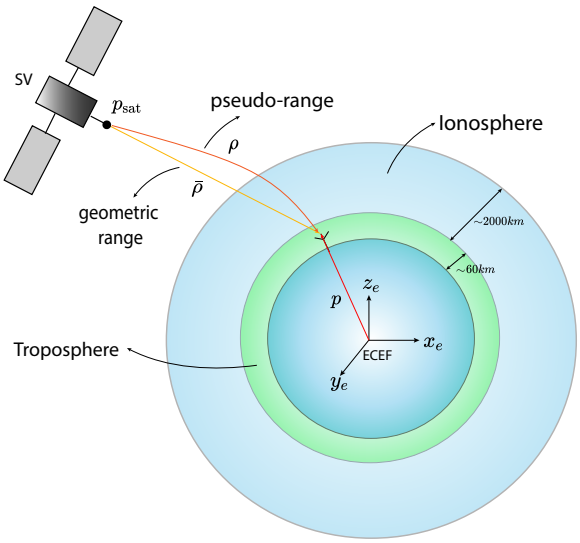

Figure 3. Earth's atmosphere consists of the ionosphere and troposphere layers. Notice the difference between the geometrical range and the pseudo-range.

using a mathematical model, for instance, the Klobuchar model for the ionospheric part and the Saastamoine model for the troposphere part (see (Grewal et al., 2013)).

Figure 3 depicts (without scale) the Earth atmosphere and the geometric versus pseudo-range distances.

Accordingly, for a set of M visible satellites, the measurement model can be written as

$$y := \begin{bmatrix} \rho^1 \\ \rho^2 \\ \vdots \\ \rho^M \end{bmatrix} = \begin{bmatrix} \|p^1_{\mathrm{sat}} - p\|_2 + c\Delta t + \Psi^1 + \epsilon^1 \\ \|p^2_{\mathrm{sat}} - p\|_2 + c\Delta t + \Psi^2 + \epsilon^2 \\ \vdots \\ \|p^M_{\mathrm{sat}} - p\|_2 + c\Delta t + \Psi^M + \epsilon^M \end{bmatrix} \tag{18}$$

with $\Psi^i = \delta\rho^i_{\mathrm{rel}} - c\Delta t^i_{\mathrm{sat}} + Tr^i + I^i + TGD^i$.

The satellite noises are assumed to be zero-mean Gaussian, i.e. $\epsilon^i \sim \mathcal{N}(0, (\sigma^2_R)^i)$ with its standard deviation in the form,

$$\sigma^i_R = a + b\exp(-c\phi^i) \tag{19}$$

where ϕ^i is the satellite elevation angle. Note that as the elevation angle decreases, the noise variance increases. This is because satellites with low elevation show higher noise intensity.

3. KINEMATIC MODEL

3.1 Nearly Constant Velocity

For GNSS applications with moving targets defining a prior kinematic model is common. The most used model is the Nearly Constant Velocity (NCV) (Bar-Shalom et al., 2001) due to its simplicity. In the Euclidean representation, it is given as,

$$\dot{p} = v \tag{20a}$$
$$\dot{v} = w \tag{20b}$$

where $p \in \mathbb{R}^3$ is the position, $v \in \mathbb{R}^3$ is the velocity, and $w \in \mathbb{R}^3$ is a zero-mean Gaussian noise. This means that the acceleration is nearly zero up to a zero-mean perturbation; hence, the model represents a nearly constant velocity target.

ISSN: 2525-8311 0727 DOI: 10.20906/CBA2022/3274

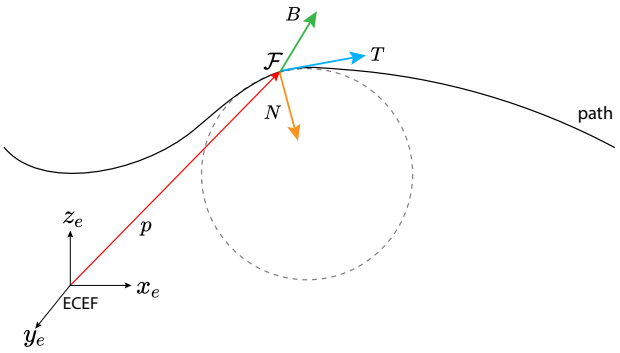

Figure 4. Frenet-Serret frame with ECEF as a reference frame.

However, the Euclidean formulation (20) disregards any geometrical property of the path. In contrast, this work, motivated by the initial studies on radar tracking presented in (Magalhães, 2021), proposes the adoption of an alternative formulation of NCV based on the Frenet-Serret frame embed on a Lie Group.

The advantage of the Frenet-Serret frame is that it allows one to model the path independently of an external coordinate system's choice and summarize the course's characteristic exclusively through two scalar parameters: curvature κ and torsion τ.

The Frenet-Serret frame is defined by a tangent vector $T \in \mathbb{R}^3$, a normal vector $N \in \mathbb{R}^3$, and a bi-normal vector $B \in \mathbb{R}^3$. Let $\mathcal{F} = [T\ N\ B]^\intercal$. Thus, the Frenet-Serret dynamic model in compact form can be stated as

$$\frac{d\mathcal{F}}{ds} = \begin{bmatrix} 0 & \kappa & 0 \\ -\kappa & 0 & \tau \\ 0 & -\tau & 0 \end{bmatrix} \mathcal{F}. \tag{21}$$

Accordingly, the position of a target can be determined by the position of the Frenet-Serret frame in space regarding a reference frame. For GNSS, the Earth-Centered-Earth-Fixed (ECEF) is the most convenient reference frame, as all satellite measurements are available in this frame.

Figure 4 illustrates the Frenet-Serret frame with the ECEF as reference. It is important to stress that the orientation of the Frenet-Serret frame is not necessarily the body frame, which defines the target's attitude. There is no information about the target attitude in GNSS-only navigation with a single antenna.

For the nearly constant velocity scenario, as described in (Magalhães, 2021), one has $\tau = \kappa = 0$, which results in the following kinematic equations

$$\dot{C} = C[w_c^\times], \tag{22a}$$
$$\dot{p} = Ce_1 v_s + Ce_1 w_v, \tag{22b}$$
$$\dot{v}_s = w_a \tag{22c}$$

where $C \in SO(3)$ is the rotation matrix from the Frenet-Serret to the ECEF frame, $p = [x_r\ y_r\ z_r]^\intercal \in \mathbb{R}^3$ is the receiver position in the ECEF frame, $e_1 = [1\ 0\ 0]^\intercal$, $w_c \sim \mathcal{N}(0, \sigma_c^2)$, $w_v \sim \mathcal{N}(0, \sigma_v^2)$, $w_a \sim \mathcal{N}(0, \sigma_a^2)$ are zero-mean Gaussian noises accounting for uncertainties on the Frenet-Serret orientation, velocity and acceleration, respectively. Here, $[\omega^\times]$ stands for the *skew-symmetric matrix* and for any $\omega \in \mathbb{R}^3$ is defined as

$$[\omega^\times] = \begin{bmatrix} 0 & -\omega_3 & \omega_2 \\ \omega_3 & 0 & -\omega_1 \\ -\omega_2 & \omega_1 & 0 \end{bmatrix}. \tag{23}$$

An exciting feature of the model (22) is that the velocity vector is constrained to always be tangent to the trajectory even with the noise addition.

The Lie group structure $SE(3) \times T(2)$ is adopted to represent the system state in the form

$$X = \left[\begin{array}{cc|c} C & p & 0_{4\times 3} \\ 0 & 1 & \\ \hline & & 1\ 0\ v_s \\ 0_{3\times 4} & & 0\ 1\ c\Delta t \\ & & 0\ 0\ 1 \end{array}\right]_{7\times 7} \tag{24}$$

In addition, $v_s = \|v\| \in \mathbb{R}$ is the target speed and $c\Delta t \in \mathbb{R}$ is error due to the GNSS clock receiver offset (assumed nearly constant, e.g. $c\dot{\Delta t} = w_d$ with $w_d \sim \mathcal{N}(0, \sigma_d^2)$). The respective Lie Algebra element is, thus, in the form

$$x = \begin{bmatrix} \omega \\ \theta_1 \\ \theta_2 \\ \theta_3 \end{bmatrix}^\wedge_G = \left[\begin{array}{cc|c} [\omega^\times] & \theta_1 & 0_{4\times 3} \\ 0 & 0 & \\ \hline & & 0\ 0\ \theta_2 \\ 0_{3\times 4} & & 0\ 0\ \theta_3 \\ & & 0\ 0\ 0 \end{array}\right]_{7\times 7}. \tag{25}$$

where $\omega \in \mathbb{R}^3$, $\theta_1 \in \mathbb{R}^3$, $\theta_2 \in \mathbb{R}$ and $\theta_3 \in \mathbb{R}$. It is straightforward to check that the left velocity function for this case is

$$\Omega(X, u) = [X^{-1}\dot{X}]^\vee_G = \begin{bmatrix} 0_{3\times 1} \\ e_1 v_s \\ 0_{2\times 1} \end{bmatrix}_{8\times 1}, \tag{26}$$

and the adjoint representations are

$$\mathrm{Ad}_G(X) = \left[\begin{array}{cc|c} C & 0 & 0_{6\times 2} \\ [p^\times]C & C & \\ \hline 0_{2\times 6} & & I_{2\times 2} \end{array}\right], \tag{27}$$

$$\mathrm{ad}_G(x) = \left[\begin{array}{cc|c} [\omega^\times] & 0 & 0_{6\times 2} \\ [\theta_1^\times] & [\omega^\times] & \\ \hline 0_{2\times 6} & & 0_{2\times 2} \end{array}\right]. \tag{28}$$

4. GNSS SOLUTION

After establishing the prior kinematic model for the target and the measurement model for the GNSS, the Kalman Filter can be implemented following Eq. (15).

Figure 5 shows the resulting GNSS system in action. Notice that because of the adoption of the intrinsic nearly constant velocity model, described in Section 3.1, the position prediction will present a curved-shape distribution by construction, a CGD created in the group.

ISSN: 2525-8311 0728 DOI: 10.20906/CBA2022/3274

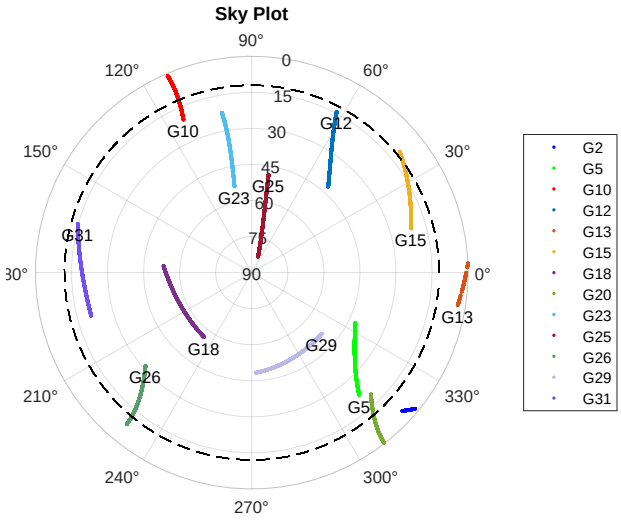

Figure 6. GPS satellites sky plot during the flight. The dashed circle indicates the 12 degrees elevation mask.

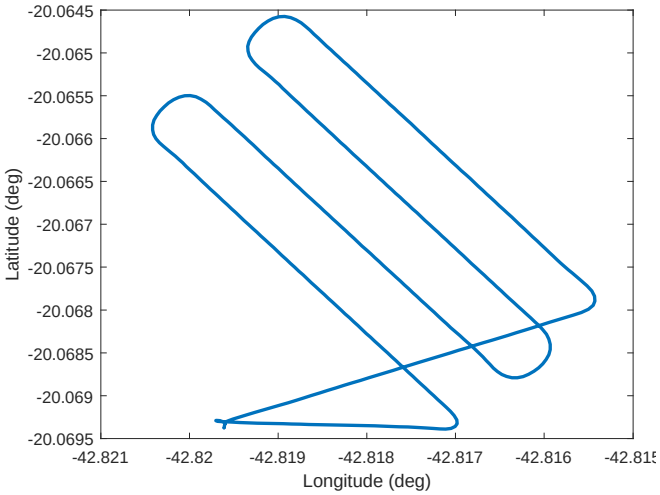

Figure 7. Horizontal flight profile.

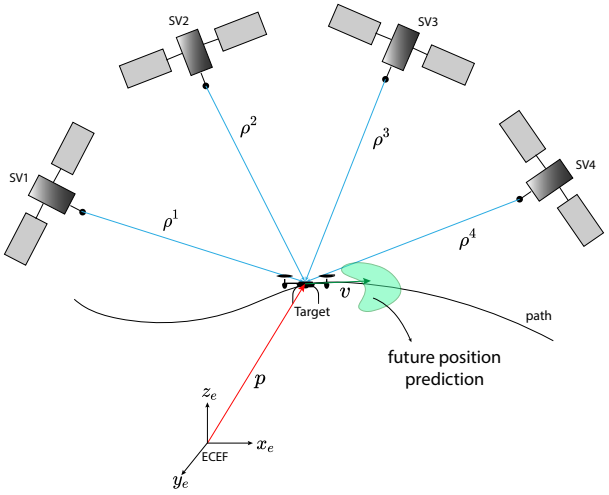

Figure 5. Simplified schematic of GNSS system using intrinsic NCV model on Lie Groups.

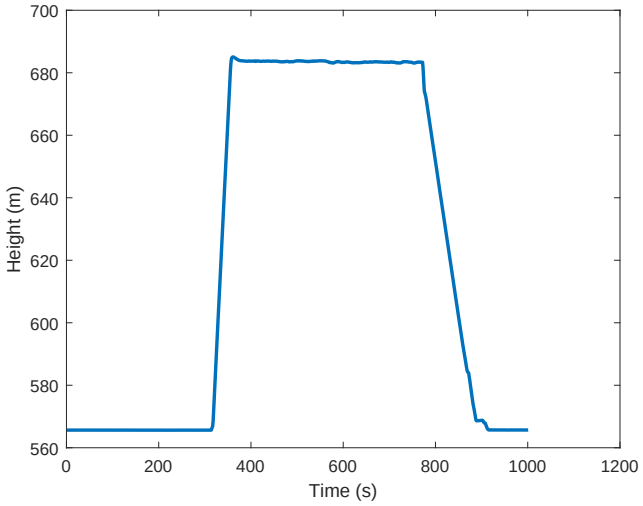

Figure 8. Vertical flight profile.

5. EXPERIMENT

In order to evaluate the performance of the proposed filtering scheme, a real dataset obtained from a hexacopter flight is employed. The data comes from a single antenna GNSS receiver ublox® ZED-F9 installed on a DJI® M600-pro hexacopter. The receiver sample rate is $1Hz$, and all data are available in raw format. For simplicity, only the GPS constellation is processed in this example.

The GPS satellite's position is computed from the broadcasted ephemeris data. Figure 6 shows the visible satellite during the entire flight. An elevation mask of 12° is applied to discard too low-elevation satellites during the filtering process. The horizontal flight profile is shown in the Figure 7 and the vertical profile in Figure 8. All parameters utilized in the filter algorithm are summarized in Table 1.

Table 1. Model parameters.

Parameter	Value
σ_a	$3^{(m/s^2)}/\sqrt{s}$
σ_v	$7^{(m/s)}/\sqrt{s}$
σ_c	$0.1^{rad}/\sqrt{s}$
σ_d	$30^{m}/\sqrt{s}$
a	0.1
b	5
c	$2/(\pi/2)$

Moreover, the filter initial covariance was set to

$$P_0 = \text{diag}((10°)^2, (10°)^2, (20°)^2, (10m)^2, (10m)^2, (10m)^2, (1m/s)^2, (1000m)^2).$$

Two filters were implemented for this comparison. One was based on the NCV model using Euclidean representation, and the second was based on the NCV using the Frenet-

ISSN: 2525-8311 0729 DOI: 10.20906/CBA2022/3274

Table 2. RMSE comparison.

ECEF	Euclidean	Lie-Group	Gain
x	1.385m	1.278m	7.70%
y	1.428m	1.210m	15.27%
z	0.966m	0.900m	6.79%
p	1.277m	1.142m	10.59%

Serret frame on Lie Groups, described in Section 3. The parameter's values from Table 1 are the same for both filters.

After processing the raw data using the Euclidean and Lie Group filters, the error against the ground truth was computed. The resulting RMSE, for each ECEF coordinate and the position vector, are shown in Table 2 with the respective performance gain. In addition, Figure 9 shows the resulting error histogram for both filters. One can notice that the red histograms (Lie Group filter) appear closer to the normal distribution and show a smaller bias than the blue one (Euclidean filter). This indicates an overall better performance of the proposed Lie Group-based filter.

6. CONCLUSION

The paper proposed, implemented, and tested an alternative formulation of the usual nearly constant velocity model for GNSS tracking. The formulation employs the Frenet-Serret frame embedded in a Lie Group, furnishing the dynamic model for a Kalman-like filter in Lie Groups. As a result, the uncertainty distribution in position becomes banana-shaped instead of ellipsoidal. This alternative formulation is more appropriate for capturing the characteristics of a rigid body performing simultaneous translations and rotations in space, such as drones and airplanes. A numeric experiment using raw data from an actual GNSS receiver shows that the NCV Lie Group-based approach yields better results (about 10% in position RMSE) than the usual Euclidean method. The results demonstrate that the proposed filtering scheme is applicable for real scenarios and could help improve satellite-based navigation systems.

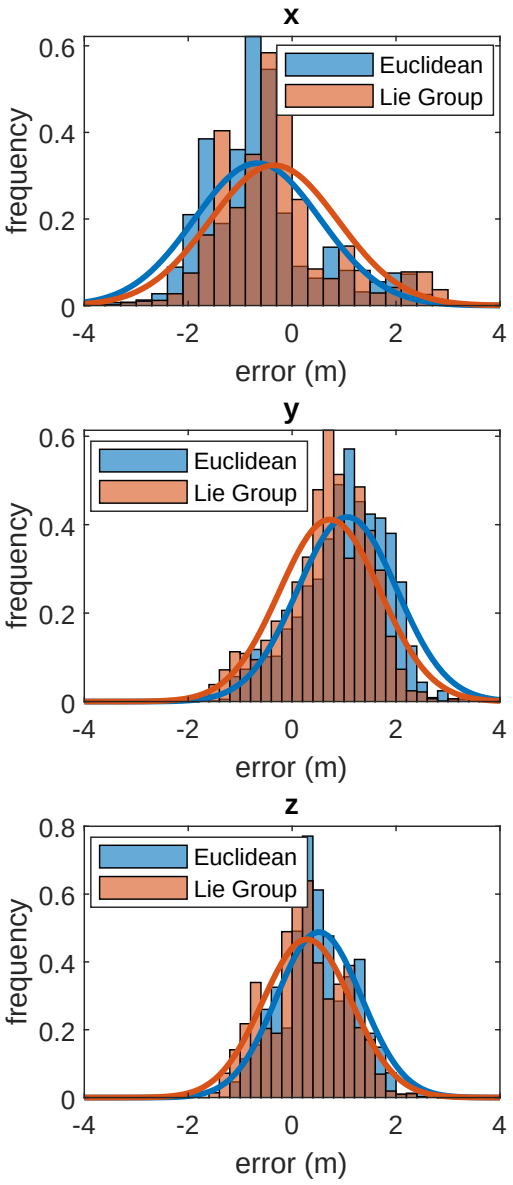

Figure 9. Error histogram of each ECEF coordinate. Notice that, for each coordinate, the red histogram is slightly closer to a normal distribution compared with the blue histogram, indicating a better estimation performance.

ACKNOWLEDGEMENTS

This work was supported in part by the Coordenação de Aperfeiçoamento de Pessoal de Nível Superior (CAPES), Brazil Finance Code 001 under Grant 88887.342183/2019-00; in part by the Conselho Nacional de Desenvolvimento Científico e Tecnológico (CNPq) under Grant 303352/2018; and in part by FAPESP under Grant 2016/08645-9.

The authors would like to thank the Radaz Indústria e Comércio de Produtos Eletrônicos S.A. for providing the GNSS data for this work.

REFERENCES

Bar-Shalom, Y., Li, X.R., and Kirubarajan, T. (2001). *Estimation with Applications To Tracking and Navigation*, volume 9. John Wiley & Sons.

Barczyk, M. and Lynch, A.F. (2013). Invariant observer design for a helicopter UAV aided inertial navigation system. *IEEE Transactions on Control Systems Technology*, 21(3), 791–806.

Barrau, A. and Bonnabel, S. (2020). Extended Kalman Filtering with Nonlinear Equality Constraints: A Geometric Approach. *IEEE Transactions on Automatic Control*, 65(6), 2325–2338. doi:10.1109/TAC.2019.2929112.

Barrau, A. and Bonnabel, S. (2018). Invariant Kalman Filtering. *Annual Review of Control, Robotics, and Autonomous Systems*.

Bourmaud, G., Giremus, A., Berthoumieu, Y., and Bourmaud, G. (2013). Discrete extended Kalman filter on lie groups. In *21st European Signal Processing Conference*. Marrakech, Morocco.

Bourmaud, G., Mégret, R., Arnaudon, M., and Giremus, A. (2014). Continuous-Discrete Extended Kalman Filter on Matrix Lie Groups Using Concentrated Gaussian Distributions. *Journal of Mathematical Imaging and Vision*, 51(1), 209–228.

Bourmaud, G., Mégret, R., Giremus, A., and Berthoumieu, Y. (2016). From Intrinsic Optimization to Iterated

ISSN: 2525-8311 0730 DOI: 10.20906/CBA2022/3274

Extended Kalman Filtering on Lie Groups. *Journal of Mathematical Imaging and Vision*, 55(3), 284–303.

Chirikjian, G. (2011). *Stochastic Models, Information Theory, and Lie Groups - vol2*. Springer Science+Business Media.

Cui, J. (2021). Lie group based nonlinear state errors for MEMS-IMU / GNSS / magnetometer integrated navigation. *The Journal of Navigation*, 1–14.

Farrell, J.A. (2008). *Aided Navigation Systems: GPS and High Rate Sensors*. McGraw-Hill.

Grewal, M.S., Andrews, A.P., and Bartone, C.G. (2013). *Global Navigation Satellite Systems, Inertial Navigation, and Integration*. Wiley, 3th edition.

Groves, P.D. (2013). *Principles of GNSS, Inertial, and Multisensor Integrated Navigation Systems 2nd*. Artech House.

Hall, B. (2007). *Lie Groups, Lie Algebras and Representations: An Elementary Introduction*. Springer.

Long, A.W., Wolfe, K.C., Mashner, M.J., and Chirikjian, G.S. (2012). The Banana Distribution Is Gaussian: A Localization Study with Exponential Coordinates. In *Robotics: Science and Systems*.

Magalhães, G.d.M. (2021). Radar aerial target-tracking on Lie groups. *Master Thesis, UNICAMP*.

Magalhães, G.D.M., Dranka, E., Cáceres, Y., Do Val, J.B., and Mendes, R.S. (2018). EKF on Lie Groups for radar tracking using polar and Doppler measurements. In *2018 IEEE Radar Conference, RadarConf 2018*, volume 1573, 1573–1578.

Pulford, G.W. (2010). Analysis of a nonlinear least squares procedure used in global positioning systems. *IEEE Transactions on Signal Processing*, 58(9), 4526–4534. doi: 10.1109/TSP.2010.2050061.

Sahmoudi, M. and Landry, R. (2009). A nonlinear filtering approach for robust Multi-GNSS RTK positioning in presence of multipath and ionospheric delays. *IEEE Journal on Selected Topics in Signal Processing*, 3(5), 764–776. doi:10.1109/JSTSP.2009.2033158.

Subirana, J., Zornoza, J., and Hernández-Pajares, M. (2013). *Gnss Data Processing*, volume I. ESA Communications.

Takasu, T. and Yasuda, A. (2007). Development of the low-cost rtk-gps receiver with an open-source program package rtklib. *Conference*.

ISSN: 2525-8311 0731 DOI: 10.20906/CBA2022/3274